IJIRSET
International Journal of Innovative Research in Science | Engineering | Technology

ISSN(O): 2319-8753
ISSN(P): 2347-6710

International Journal of Innovative Research in Science Engineering and Technology (IJIRSET)

(A Monthly, Peer Reviewed, Refereed, Scholarly Indexed, Open Access Journal)

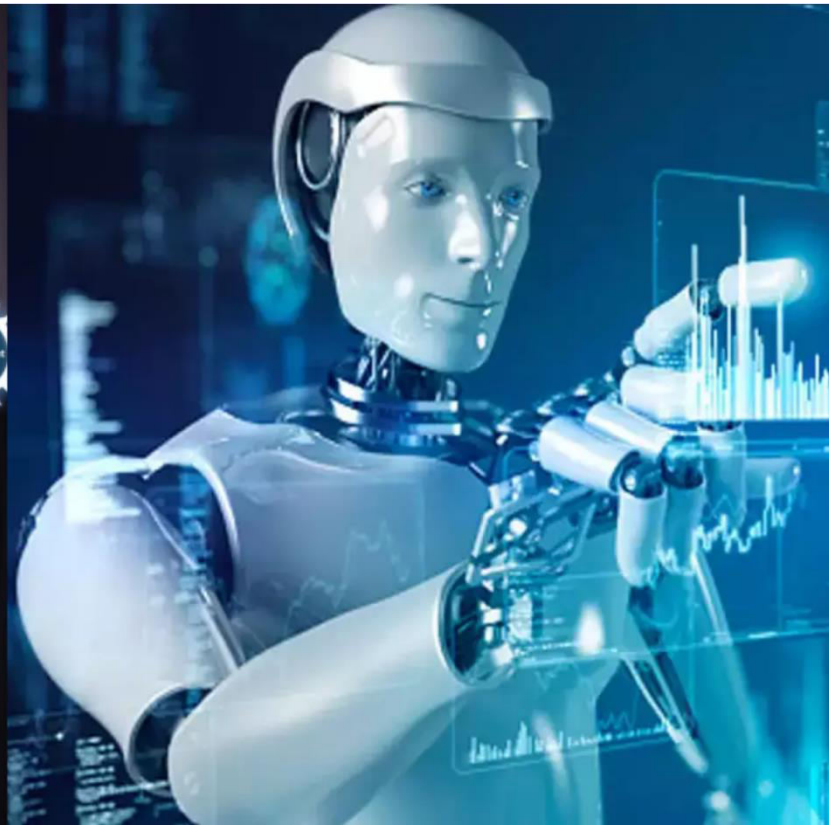

Impact Factor: 8.699

Volume 14, Issue 8, August 2025

International Journal of Innovative Research of Science, Engineering and Technology (IJIRSET)

Impact Factor 8.699

|www.ijirset.com |A Monthly, Peer Reviewed & Refereed Journal| e-ISSN: 2319-8753| p-ISSN: 2347-6710|

Volume 14, Issue 8, August 2025

|DOI: 10.15680/IJIRSET.2025.1408061|

Advanced Imaging Techniques for the Classification of Covid-19 by Modified Harmony Search Based Sine Cosine Algorithm (MHS-SCA)

Dr. S. Joseph Jawhar[1*], Dr. C. Agees Kumar[2]

Department of Electrical and Electronics Engineering, Arunachala College of Engineering for Women, Manavilai, Nagercoil, Tamil Nadu, India[1]

Department of Electrical and Electronics Engineering, Arunachala College of Engineering for Women, Manavilai, Nagercoil, Tamil Nadu, India[2]

*Corresponding author

ABSTRACT: Computer-aided diagnosis has become an essential tool for the precise and prompt detection of coronavirus disease (COVID-19), which is necessary to reduce the burden on the healthcare system during the pandemic and prevent the virus from spreading. A vast number of investigations on COVID-19 detection using a smaller set of original X-ray pictures have been published. Nonetheless, there is no literature on the influence of lung segmentation and image enhancement on COVID-19 detection over a large dataset. The data were acquired from the Kaggle Dataset. Adaptive Median Filter (AMF) methods are initially used for image preparation. The pre-processed images are then segmented with the Markov Random Field (MRF) modeling technique. Feature extraction is performed on the extracted segments. The feature data is extracted using the Linguistic Neuro-Fuzzy with Feature Extraction model (LNF-FE). used to look into how image enhancing methods affect the detection of COVID-19. The proposed research uses the Modified Harmony Search Based Sine Cosine Algorithm (MHS-SCA) architecture to classify as “NORMAL” or “COVID 19”. The suggested MHS-SCA model provides enhanced precision and a higher rate of accurately classifying brain tumors.

KEYWORDS: Adaptive Median Filter; coronavirus; Markov Random Field; healthcare system.

I. INTRODUCTION

The epidemic of COVID-19 has put global public health at considerable risk. A seafood market in Wuhan City, Hubei Province, China, in December 2019 exposed individuals to the severe acute respiratory syndrome coronavirus 2 (SARS-CoV-2) were the first to be isolated and found to be the cause of COVID-19. COVID-19 is a pandemic of unprecedented magnitude in recent human history. Four million people have died and around 200 million illnesses have been confirmed worldwide in less than 18 months after the outbreak started. The availability of education at all levels has increased dramatically during the past 50 years on a global scale. The biggest threat to these enlarged national education systems has never been COVID-19. Many governments have compelled universities to discontinue face-to-face instruction for the majority of its students, forcing them to transition almost immediately to online teaching and virtual education [1]. The data set includes chest x-rays from healthy people as well as those diagnosed with COVID-19 or viral pneumonia. The data set underwent the data augmentation procedure before the classification stage [2]. Examines various image pre-processing techniques for COVID-19 automatic detection using CT scans. To remove blood vessel spots, consider using a smoothing picture approach based on Median and Gaussian filters [3]. However, CXR's sensitivity in detecting COVID-19 may be lower. This study proposes a deep learning framework for accurate COVID-19 categorization and severity prediction based on CXR images. U-Net is used for lung segmentation and has an accuracy of 0.9924 [4]. M aximizes the detection of COVID-19 by utilizing seven convolutional neural networks: MobileNetV2, DenseNet121, InceptionV3, ResNet50V2, Xception, EfficientNet-B0, and EfficientNetV2. Additionally, using a small set of chest X-ray and CT pictures, the lightweight convolutional neural network LightEfficientNetV2 may achieve an accuracy and F1-Score of 98.5% [5]. The MobileNet structure uses a linear kernel with the SVM

International Journal of Innovative Research of Science, Engineering and Technology (IJIRSET)

Impact Factor 8.699

|www.ijirset.com |A Monthly, Peer Reviewed & Refereed Journal| e-ISSN: 2319-8753| p-ISSN: 2347-6710|

Volume 14, Issue 8, August 2025

|DOI: 10.15680/IJIRSET.2025.1408061|

classifier. For the different dataset, the best pairing is DenseNet201 with MLP, which achieves an accuracy and F1-Score of 95.6%. Thus, the suggested approach effectively detects COVID-19 in X-ray pictures [6].

Contribution of this Work

For more details, the following are the main stages of the recommended strategy:

1. A high-performing Initial and accurate Covid 19 classification using a MHS-SCA architecture based Deep learning system.
2. The pre-processing stage is done through a AMF, to improve the quality of image.
3. Then applied a Markov Random Field (MRF) segmentation for segmenting the chest X rays.
4. The feature will be extracted using Linguistic Neuro-Fuzzy with Feature Extraction (LNF-FE) model.
5. A Deep learning based MHS-SCA architecture is used and optimized for classification of Covid 19 and normal is proposed. Precision, sensitivity, and specificity are used to evaluate how well the suggested strategy performs.

The following describes how the document is established. Section 1 displays the introduction. Section 2 describes the relevant works. Section 3 discusses the proposed methodologies, Section 4 summarizes the experiment's outcomes, and Section 5 provides a conclusion and future study.

II. LITERATURE REVIEW

Lamsal et al. [7] have proposed, the GeoCOV19Tweets Dataset the geo version of the dataset, and analyzes the tweets in both datasets. The datasets are made publicly available in the hopes of improving our understanding of the temporal and spatial dimensions of public discourse surrounding the ongoing pandemic. Tabik et al. [8] have suggested, COVID-19 attitude and emotion analysis through social media; and (d) COVID-19 case reporting, transmission estimation, and prognosis based on epidemiological, demographic, and mobility data. Heidari et al. [9] have discussed, a bilateral low-pass filter and a histogram equalization approach were used to process the original image. The original image and two filtered images are blended to produce a false color image. This image is fed into three input channels of a transfer learning-based convolutional neural network (CNN) model to classify chest X-ray images into three categories: COVID-19-infected pneumonia, other pneumonia acquired in the community that is not COVID-19-infected, and normal (non-pneumonia) cases. Das et al. [10] have recommended, a World in Data (OWID) dataset was used to evaluate the impact of a customized data pretreatment pipeline on ten machine learning models that predicted COVID-19 mortality. The pipeline differs from standard preprocessing pipelines in four key steps. Li et al. [11] have reported, CDRIME-MTIS is a novel multi-threshold image segmentation method that combines the 2D non-local histogram with the 2D Kapur entropy. The segmentation experiments utilizing COVID-19 X-ray images show that CDRIME performs better than RIME and its competitors in terms of threshold level adaptability and segmentation effect.

Sharma et al. [12] have described, there are 16 different types of segmentation-based classification deep learning systems that can detect COVID-19 automatically, fast, and precisely. Eight classification models (VGG16, VGG19, Xception, InceptionV3, Densenet201, NASNetMobile, Resnet50, and MobileNet) and two deep learning-based segmentation networks (UNet and UNet+) were employed to identify the best network combination. Saygili et al. [13] have proposed, an Computer-aided diagnostic methods are being developed to help identify positive COVID-19 cases. The gold standard for virus detection at the moment is the RT-PCR assay. Due to the significant false-negative rate and result delays of the test, alternative solutions are sought. Dhebe et al. [14] have suggested, to detect COVID-19 using chest X-ray pictures. The convolutional neural network (CNN) retrieved information from X-ray pictures to construct the classification model through CNN training. The most accessible and cost-effective alternative is a chest X-ray. This study presents a Deep Convolutional Neural Network-based approach for detecting COVID-19 positive patients using chest X-Ray pictures. Multiple cutting-edge CNN models.

Gursoy et al. [15] have recommended, the COVID-19 detection methods are divided into two areas, and investigations are discussed. Second, the reported publicly available datasets, their attributes, and potential comparison materials described in the literature are presented. Third, a comprehensive comparison is made by examining the similarities and differences between the studies. Finally, the study summarizes the findings, gaps, and limits to encourage the development of COVID-19 detection methods, and it finishes with a list of future research topics for COVID-19 categorization. Thakur et al. [16] have described, a Covid-19 diagnosis for patients has become critical. The aim of this

International Journal of Innovative Research of Science, Engineering and Technology (IJIRSET)

Impact Factor 8.699

|www.ijirset.com |A Monthly, Peer Reviewed & Refereed Journal| e-ISSN: 2319-8753| p-ISSN: 2347-6710|

Volume 14, Issue 8, August 2025

|DOI: 10.15680/IJIRSET.2025.1408061|

study is to use X-ray and to deploy a deep learning technique based on the CNN to automatically identify and detect the Covid-19 disease.

Zouch et al. [17] have proposed, to develop a novel approach for automatically detecting COVID-19 using tomographic (CT) and radiographic images (Chest X-ray). To improve the detection system's performance during this outbreak, we used two deep learning models: VGG and ResNet. The experiment results show that our proposed models achieved the highest accuracy of 99.35 and 96.77% for VGG19 and ResNet50 on all chest X-ray images. Hayat et al. [18] have suggested, X-rays can help to identify COVID-19. This study analyzed 17,599 images to develop models for classifying the occurrence of COVID-19 infection, and four different classifiers were examined. These include convolutional neural networks (SCovNet and ResNet18), support vector machines, and logistic regression. The proposed SCoVNet architecture beat all four models, with accuracy of approximately 99% and 98% on chest computed tomography scans and chest X-ray images, respectively.

III. PROPOSED SYSTEM

Figure 1 depicts the workflow of a COVID-19 detection system employing chest X-ray images, which is led by the MHS-SCA classification algorithm. The method starts with the input image, a raw chest X-ray. This image is pre-processed with an AMF to improve its quality and reduce noise. The filtered image is then segmented using MRF modeling to isolate the lung areas from the background. Following segmentation, the LNF-FE model is used to extract relevant features from the lung areas that have been segmented. These features are then passed to the MHS-SCA classifier, a hybrid optimization-based machine learning method that divides the input into two categories: normal and COVID-19. This pipeline provides accurate detection through the methodical enhancement, segmentation, feature extraction, and classification of medical images.

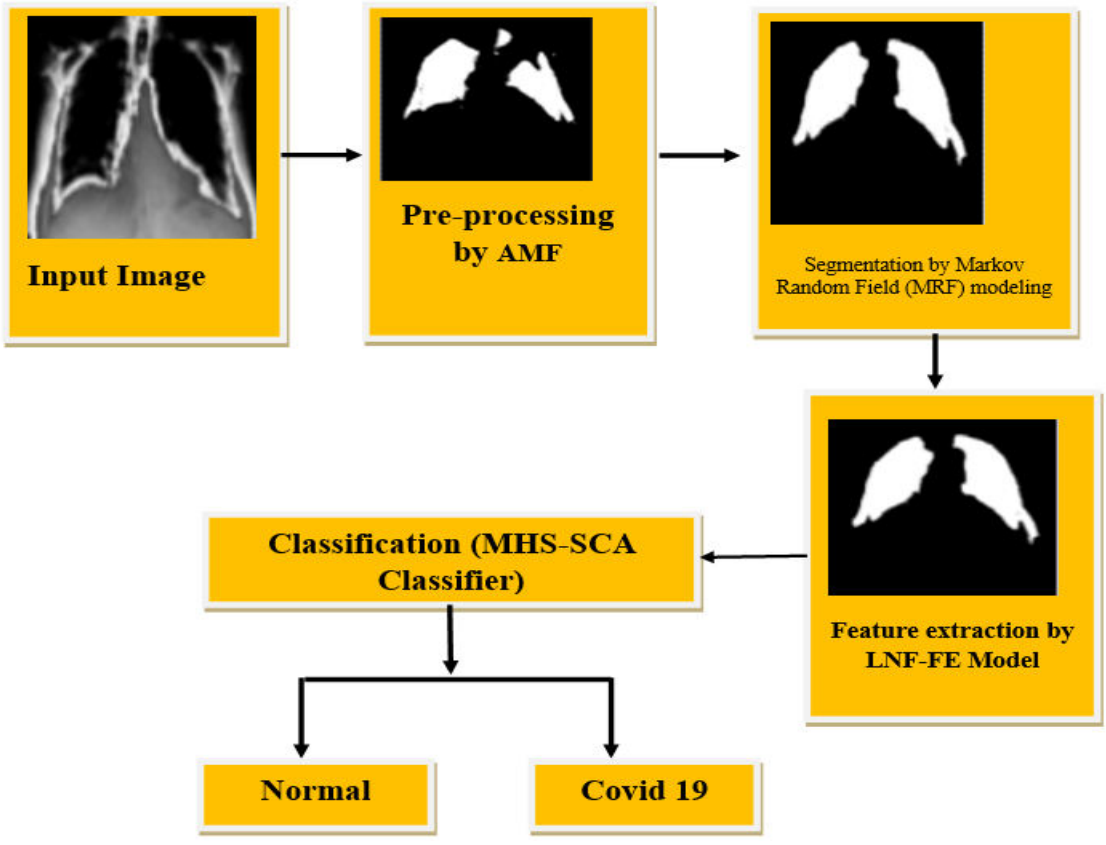

Figure 1. Flowchart for the proposed Model of Covid 19 classification

International Journal of Innovative Research of Science, Engineering and Technology (IJIRSET)

Impact Factor 8.699

|www.ijirset.com |A Monthly, Peer Reviewed & Refereed Journal| e-ISSN: 2319-8753| p-ISSN: 2347-6710|

Volume 14, Issue 8, August 2025

|DOI: 10.15680/IJIRSET.2025.1408061|

3.1Preprocessing

Only the Adaptive Median Filter is capable of doing standard median filtering. Spatial processing is used to determine if pixels in an image are prone to impulse noise. It compares adjacent pixels in a picture to see if they contain noise. It is possible to adjust both the neighborhood size and the reference threshold. Noise is defined as a pixel that differs from the majority of its neighbors but is not aligned with the pixels to which it is identical [18]. The impulse noise pixels are then replaced with the median pixel value of the neighborhood that passed the noise identification test. The adaptive median filter (AMF) function is described as follows:

1) Eliminate of any impulse noise 2) Smoothing of other noise. 3) Reduce distortion.

Even if the photos in the dataset have several intensity ranges and exceed the standard intensity value of 255, preprocessing is required. A certain set of preprocessing procedures is required to make network training efficient and quantifiable. It has been shown that preprocessing increases segmentation accuracy.

3.2Segmentation

The initial stage of Markov Random Field (MRF) modeling, as seen in Figure 3, involves defining an energy function that depicts the interaction between adjacent pixels in the picture. The energy function normally consists of two terms: the data term, which assesses how well each pixel's intensity matches its given label, and the smoothness term, which promotes smooth transitions between adjoining pixels. The mathematical expression for the energy function is as follows:

$$E(L) = \sum_i \psi_d(i, l_i) + \sum_{(i,j)\in N} \psi_s(i, l_i, l_j) \quad (1)$$

The data term is denoted by $\psi_d(i, l_i)$, the smoothness term by $\psi_s(i, l_i, l_j)$, the labeling configuration of the picture by L, the label applied to pixel I by l_i, and the set of neighboring pixel pairs by N. MRF-based segmentation employs contextual information from surrounding pixels to effectively guide the segmentation procedure. By considering the spatial correlations between pixels, the MRF component increases segmentation accuracy and resilience, particularly when dealing with complex backgrounds and noise. Mathematically, the minimization problem is expressed as,

$$L^* = \arg\min E(L) \quad (2)$$

The best labeling configuration, L ∗, reduces the energy function, E(L). At each optimization phase, the labeling configuration L is updated using the current energy function. This update takes into account both the data and smoothness terms when determining the best label for each pixel. Pixels with similar brightness and spatial closeness are more likely to be assigned the same label, resulting in coherent segmentation results. The following expression can be used to change the labeling setup mathematically:

$$l_i^{(t+1)} = \arg\min [\psi_d(i, l_i) + \sum_{j\in N_i} \psi_s(l_i, l_j^{(t)})] \quad (3)$$

Where, N_i is the set of pixels that are adjacent to i, $l_j^{(t)}$ is the label of neighboring pixel j at iteration t, and $l_i^{(t+1)}$ is the updated label for pixel i at iteration $t + 1$. Until convergence, the updating process iteratively keeps going until it finds a stable labeling configuration that minimizes the energy function.

3.3Feature Extraction

This section introduces a new hybrid model, LNF-FE, for predicting disease using medical data. This model combines the linguistic neurofuzzy model with feature extraction methods. As illustrated in Figure 2, this LNF-FE model consists of three stages: (1) fuzzification, (2) feature extraction, and (3) artificial neural network. Initially, this model converts the input qualities into linguistic values. All of these linguistic values may not always be applicable in decision-making processes. Second, a feature extraction technique is used to choose significant (reduced) features from the expanded set. Eq. (4) calculates the linguistic membership measurement for the feature Piis using the Low, Medium, and High functions for membership.

$$\mu(P_i) = [\mu_{low}(P_i), \mu_{medium}(P_i), \mu_{high}(P_i)] \quad (4)$$

International Journal of Innovative Research of Science, Engineering and Technology (IJIRSET)

Impact Factor 8.699

|www.ijirset.com |A Monthly, Peer Reviewed & Refereed Journal| e-ISSN: 2319-8753| p-ISSN: 2347-6710|

Volume 14, Issue 8, August 2025

|DOI: 10.15680/IJIRSET.2025.1408061|

Similarly, Eq. (4) computes all of the PID dataset's characteristics, which are then enlarged by Eq. (5).

$$EF_i = [\mu(P_i), \mu(G_i), \mu(BP_i), \mu(ST_i), \mu(I_i), \mu(BMI_i), \mu(DPF_i), \mu(A_i)] \quad (5)$$

The i-th instance of the expanded features (EF_i) has three times the number of membership values as the original input features. The additional feature collection complicates the model and requires more computational time to train. To solve this issue, FE algorithms are used to speed up the classification process by extracting only the most important information. FE methods, like as ICA and PCA, are employed to minimize the extended input features [19]. At this point, the fuzzified expanded membership matrix EF is put into the FE algorithm to reduce the dimension of the features.

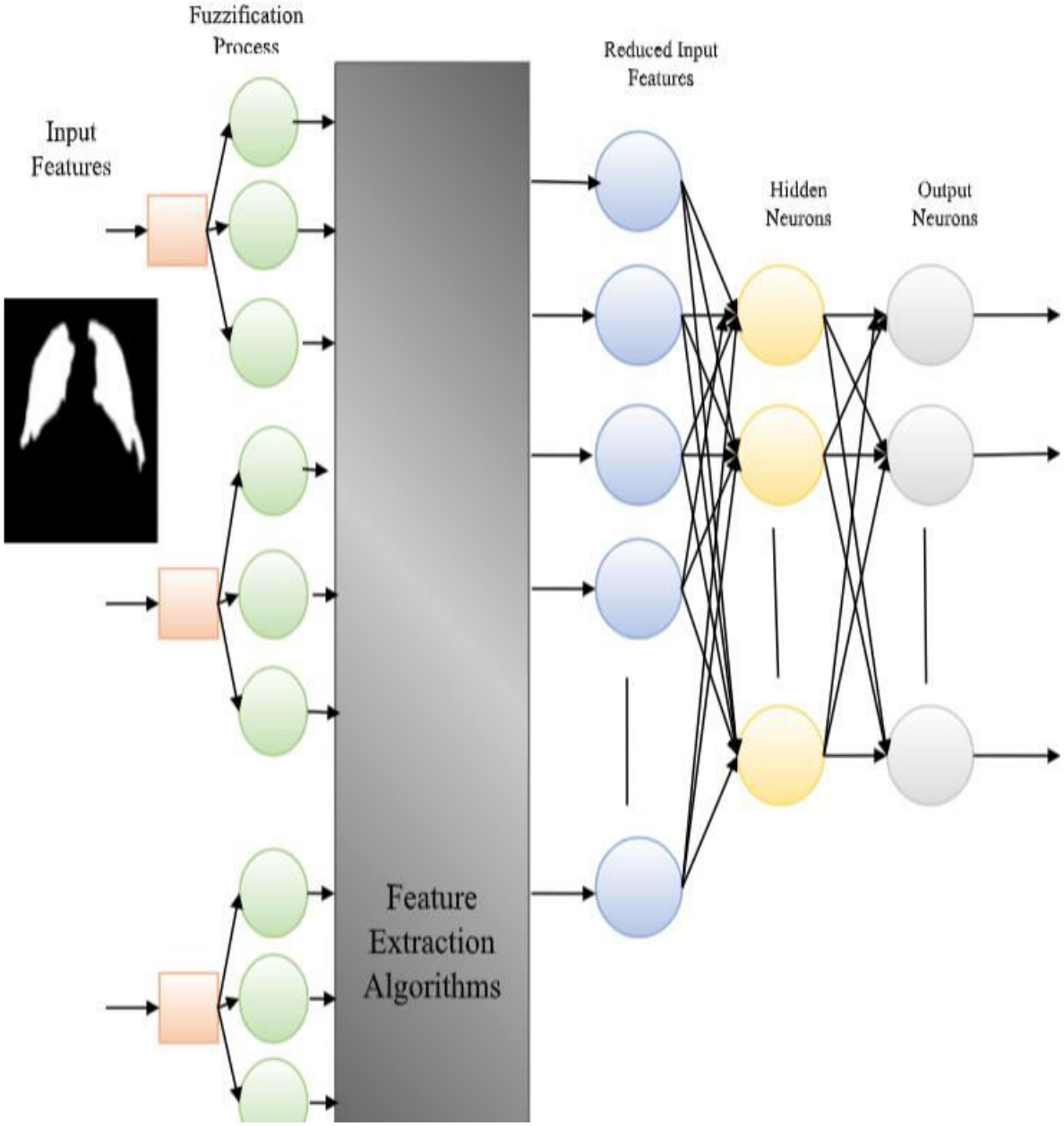

Figure 2. LNF-FE feature extraction model

International Journal of Innovative Research of Science, Engineering and Technology (IJIRSET)

Impact Factor 8.699

|www.ijirset.com |A Monthly, Peer Reviewed & Refereed Journal| e-ISSN: 2319-8753| p-ISSN: 2347-6710|

Volume 14, Issue 8, August 2025

|DOI: 10.15680/IJIRSET.2025.1408061|

3.4 MHS-SCA Optimization model for Classification

An enhanced version of the original HS method, the modified harmony search (MHS) algorithm, addressed the sluggish convergence rate and propensity to become trapped in local optima of the original HS algorithm. To achieve faster optimization, the harmony variable is set as follows:

$$z_{MHMSi}^{New}(n+1) = z_{MHMSi}^{Old}(n) + (z_i^1 - z_i^2) \times (rand), with\ PAR, \quad (6)$$

$$z_{MHMSi}^{New}(n+1) = z_{MHMSi}^{Old}(n) + (z_i^1 - z_i^2) \times X \times (rand), with\ (1 - PAR), \quad (7)$$

While χ is the learning parameter, MHMS is an acronym for modified harmony search. A higher PAR probability in the early iterations aids in the modification of numerical variables during the pitch phases, increasing the variety of solutions and avoiding local optimums, according to the PAR parameter. The PAR is provided by:

$$PAR = exp(\frac{It}{NI}) \quad (8)$$

Where, It is the most iterations, and NI is the most improvisations. A higher value for the PAR parameter must be selected. By combining the sine and cosine algorithm position equation with the harmony vector equation, the new position equation is now produced.

$$z_{MHS-SCA}^{New}(n+1) = \begin{cases} z_{MHS-SCA}^{Old}(n) + \alpha_1 \, sin\Big((z_i^1 - z_i^2) \times (\alpha_2)\Big) \times |\alpha_3 P^{gbest} - z_i^n|, & with\ PAR \\ z_{MHS-SCA}^{Old}(n) + \alpha_1 \, cos\Big((z_i^1 - z_i^2) \times (\alpha_2)\Big) \times |\alpha_3 P^{gbest} - z_i^n| \end{cases} \quad (9)$$

$$z_{MHS-SCA}^{New}(n+1) = \begin{cases} z_{MHS-SCA}^{Old}(n) + X \times \alpha_1 \, sin\Big((z_i^1 - z_i^2) \times (\alpha_2)\Big) \times |\alpha_3 P^{gbest} - z_i^n|, & with\ (1 - PAR) \\ z_{MHS-SCA}^{Old}(n) + X \times \alpha_1 \, cos\Big((z_i^1 - z_i^2) \times (\alpha_2)\Big) \times |\alpha_3 P^{gbest} - z_i^n| \end{cases} \quad (10)$$

The weights of the ELM model using the proposed hybrid MHS-SCA method. The suggested MHS-SCA approach optimizes five benchmark functions to illustrate its effectiveness. Algorithm 1 describes the pseudocode used to optimize MHS-SCA. Figure 3 depicts the flowchart for MHS-SCA. The complexity of initializing parameters and estimates for the MHS method is $O\ (n^2)$. The process model is $O\ (n)$ complicated.

International Journal of Innovative Research of Science, Engineering and Technology (IJIRSET)

Impact Factor 8.699

|www.ijirset.com |A Monthly, Peer Reviewed & Refereed Journal| e-ISSN: 2319-8753| p-ISSN: 2347-6710|

Volume 14, Issue 8, August 2025

|DOI: 10.15680/IJIRSET.2025.1408061|

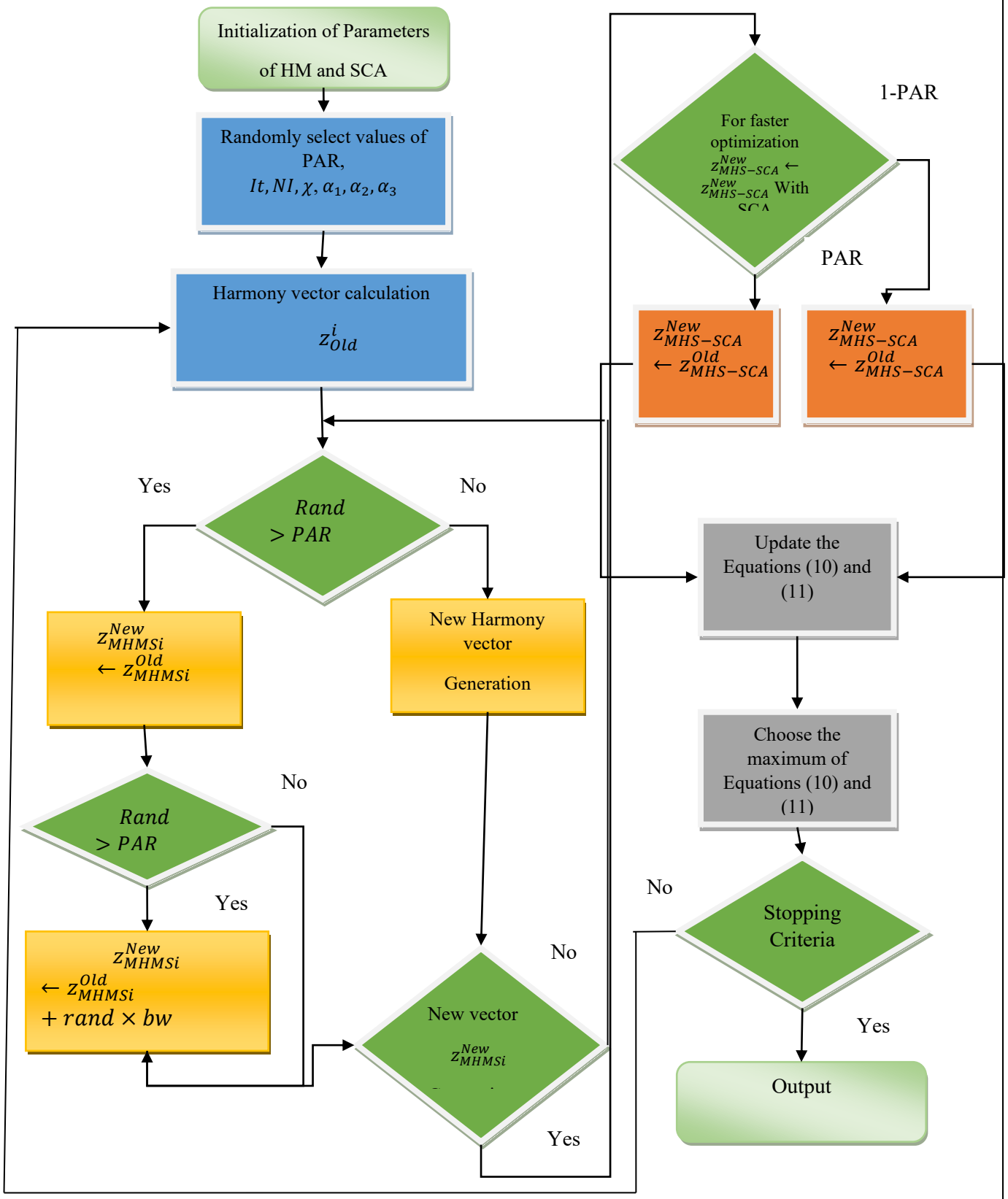

Figure 3. Flowchart for MHS-SCA algorithm

International Journal of Innovative Research of Science, Engineering and Technology (IJIRSET)

Impact Factor 8.699

|www.ijirset.com |A Monthly, Peer Reviewed & Refereed Journal| e-ISSN: 2319-8753| p-ISSN: 2347-6710|

Volume 14, Issue 8, August 2025

|DOI: 10.15680/IJIRSET.2025.1408061|

The number of calculation points employed is $2n + 1$, hence the SCA's computational complexity per time step is O (n3) [20]. The MHS-SCA computes the full calculation as $O\ (n\ log_2 n^2)$.

The output function with N hidden neurons is represent,

$$y = \sum_{n=0}^{N} \beta_n f_n(w_n; x), \qquad (11)$$

Where, $f(w;\ x) = [1, f_1(w_1;\ x), \ldots\ldots, f_n(w_n; x]$ is the hidden weight and β is the weight which can be express [21],

$$F\beta = y, \qquad (12)$$

Where, F is "feature-mapping matrix".

Algorithm 1: Pseudocode for MHS-SCA optimization algorithm

1) Set up the search parameters for harmony PAR, It, NI, χ
2) Set up the SCA's parameters $\alpha_1, \alpha_2, \alpha_3, \alpha_4$
3) determine the harmony vector by using z_{New}^{i}
4) Evaluate fitness functions using $z_{MHS-SCA}^{New}$
5) The optimization loop %
6) For $i = 1{:}\,n$
7) Use equation (8) to update the SCA parameter and obtain the ftness value.
8) Update the HS parameter $PAR = exp(It/NI)$
9) Update the modified position equation,
10)
$$z_{MHS-SCA}^{New}(n+1) = \begin{cases} z_{MHS-SCA}^{Old}(n) + \alpha_1 \sin\left((z_i^1 - z_i^2) \times (\alpha_2)\right) \times |\alpha_3 P^{gbest} - z_i^n|, \ with\ PAR \\ z_{MHS-SCA}^{Old}(n) + \alpha_1 \cos\left((z_i^1 - z_i^2) \times (\alpha_2)\right) \times |\alpha_3 P^{gbest} - z_i^n| \end{cases}$$
$$z_{MHS-SCA}^{New}(n+1) = \begin{cases} z_{MHS-SCA}^{Old}(n) + X \times \alpha_1 \sin\left((z_i^1 - z_i^2) \times (\alpha_2)\right) \times |\alpha_3 P^{gbest} - z_i^n|, \quad with\ (1 - PAR) \\ z_{MHS-SCA}^{Old}(n) + X \times \alpha_1 \cos\left((z_i^1 - z_i^2) \times (\alpha_2)\right) \times |\alpha_3 P^{gbest} - z_i^n| \end{cases}$$
11) Choose the maximum optimized z New
12) MHS−SCA values between equations (9) and (10)
13) end for the loop i
14) Stopping criteria: Converge to optimal solution, otherwise proceed to step 6.
14) Stopping criteria: Converge to optimal solution, otherwise proceed to step 6.

3.5 Evaluation matrix - COVID classification

Six performance criteria were used to assess the various CNNs' classification ability: weighted F1 score using Equations, weighted specificity, weighted precision, weighted sensitivity or recall, and total accuracy. The precision and recall weighted average is called the F1-score. Numbers 13, 14, 15, 16, 17, and 18 show the mathematical expressions for these metrics.

$$Accuracy\ = \frac{TP+TN}{TP+FP+TN+FN} \qquad (13)$$

$$Precision\ = \frac{TP}{TP+FP} \qquad (14)$$

$$Yenden's\ index\ = \frac{TP\ X\ TN\ -FN\ X\ FP}{(FP+FN)\ X\ (TN+FP)} \qquad (15)$$

$$Sepecificity = \frac{TP}{TP+FP} \qquad (16)$$

$$sensitivity(recall)\ = \frac{TP}{TP\ +FN} \qquad (17)$$

International Journal of Innovative Research of Science, Engineering and Technology (IJIRSET)

Impact Factor 8.699

|www.ijirset.com |A Monthly, Peer Reviewed & Refereed Journal| e-ISSN: 2319-8753| p-ISSN: 2347-6710|

Volume 14, Issue 8, August 2025

|DOI: 10.15680/IJIRSET.2025.1408061|

$$F1 - Score = 2\,x\,\frac{recall\ x\ precision}{recall+precision} \qquad (18)$$

IV. RESULT AND DISCUSSION

This section explains the investigative findings achieved using the recommended technique. The MHS-SCA classifier is used to categorize Covid 19. MATLAB is used to accomplish the suggested approach. This particular computer has an Intel Core i5 processor, Windows 11, 5GB of RAM, and 124GB of RAM.

4.1 Dataset

The Chest X-ray image dataset used in this study was obtained from https://www.kaggle.com/datasets/prashant268/chest-xray-covid19-pneumonia/Kaggle dataset. The dataset is divided into two folders: train and test, each with two subfolders (COVID19 and NORMAL) [22]. The dataset contains 6432 x-ray images, with test data comprising 20% of the total images. The COVID 19 identification results of the MHS-SCA approach are validated against the 10000-case database given in Table 1.

Table 1. Details about the database

True Label \ Predicted Label	Normal	COVID-19
Normal	497	3
COVID-19	4	496

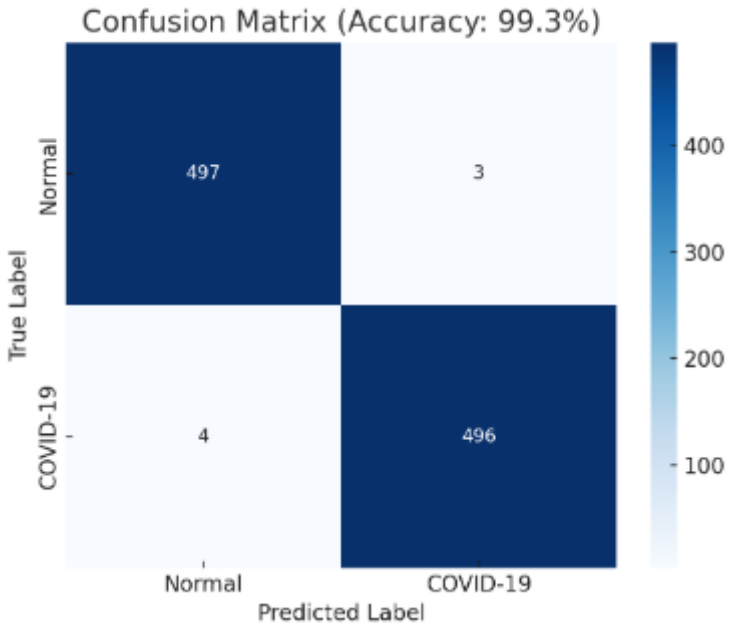

Figure 4 : Confusion Matrix

The Figure 4 shows a confusion matrix that assesses the effectiveness of a binary classification model that distinguishes between "Normal" and "COVID-19" situations, with an overall accuracy of 99.3%. The matrix indicates that 497 of 500 genuine Normal cases were accurately diagnosed, while three were incorrectly classified as COVID-19. Similarly, 496 of 500 genuine COVID-19 cases were accurately identified, whereas four were incorrectly labeled as Normal. The high accuracy and low misclassification rate indicate that the model is highly effective at discriminating between the two groups, implying a robust diagnostic capability for COVID-19 identification.

International Journal of Innovative Research of Science, Engineering and Technology (IJIRSET)

Impact Factor 8.699

|www.ijirset.com |A Monthly, Peer Reviewed & Refereed Journal| e-ISSN: 2319-8753| p-ISSN: 2347-6710|

Volume 14, Issue 8, August 2025

|DOI: 10.15680/IJIRSET.2025.1408061|

The Figure 5 depicts the accuracy curve of the proposed MHS-SCA algorithm across 25 training epochs, highlighting both training and validation accuracy. Initially, the training accuracy is around 60%, but it rapidly improves, surpassing 90% within a few epochs. It gradually increases, eventually reaching close to 99.3%, suggesting that the model fits the training data quite well.

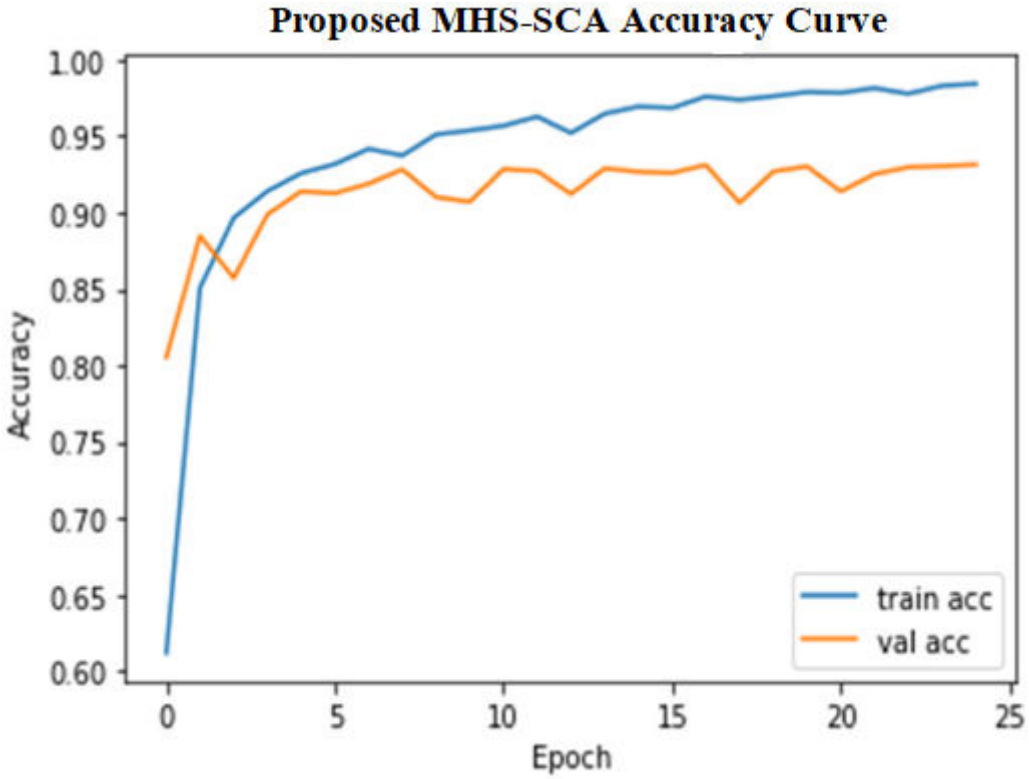

Figure 5. Accuracy curve of MHS-SCA methodology

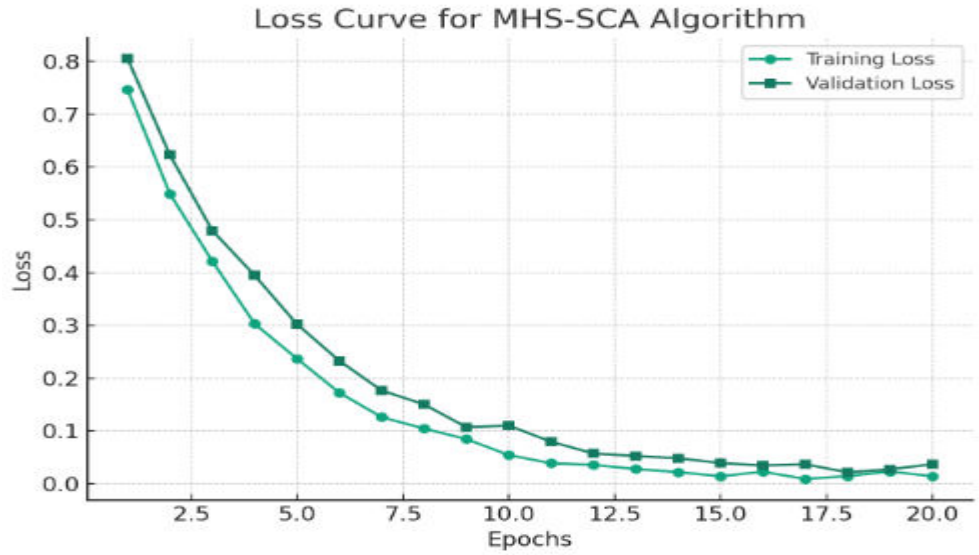

Figure 6. Loss curve of MHS-SCA methodology

International Journal of Innovative Research of Science, Engineering and Technology (IJIRSET)

Impact Factor 8.699

|www.ijirset.com |A Monthly, Peer Reviewed & Refereed Journal| e-ISSN: 2319-8753| p-ISSN: 2347-6710|

Volume 14, Issue 8, August 2025

|DOI: 10.15680/IJIRSET.2025.1408061|

The Figure 6 shows the MHS-SCA algorithm's loss curve, which depicts training and validation loss over 20 epochs. Initially, both the training and validation losses are large, around 0.8, indicating a high mistake rate at the beginning of training. As training advances, both losses rapidly decrease in the early epochs, indicating that the model is learning successfully. Around epoch 10, the losses stabilize and begin to fall more gradually, approaching near-zero levels. This indicates that the model is converging effectively without overfitting, as indicated by the near alignment of training and validation losses throughout the training period. Overall, the plot shows that the MHS-SCA method was successfully trained with minimum generalization errors.

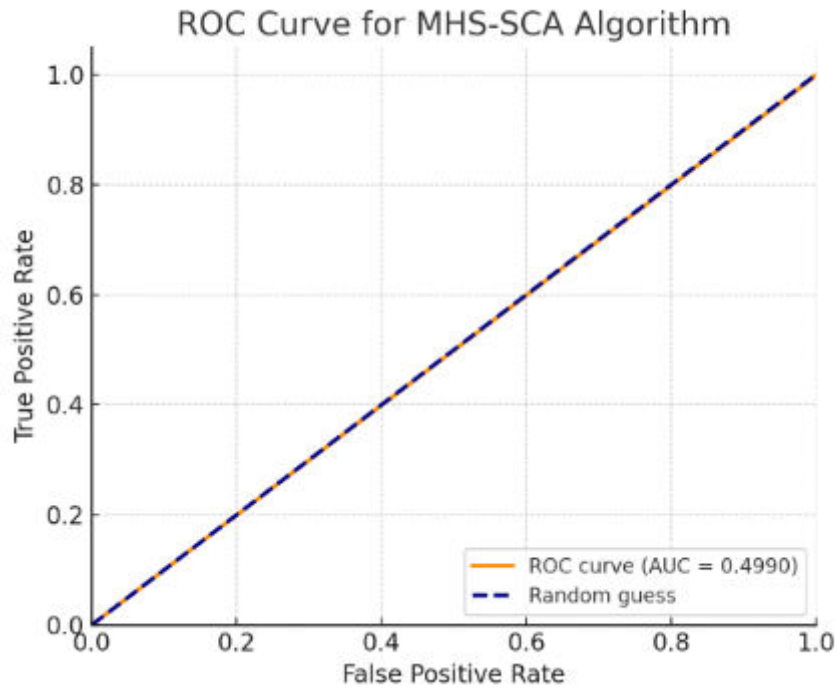

Figure 7. ROC curve of MHS-SCA methodology

Figure 7 depicts the ROC (Receiver Operating Characteristic) curve for the MHS-SCA approach, which is used to evaluate classifier performance. The ROC curve compares TPR and FPR at various threshold values. In this case, the orange curve reflecting the model's performance almost perfectly matches the diagonal blue dashed line labeled "Random guess." The AUC is reported at 0.4990, which is nearly 0.5 times the predicted AUC for a random classifier. This result shows that the model does not outperform random guessing when it comes to class distinction. Table 2 displays the comparative results of the proposed MHS-SCA approach with existing systems.

Table 2. Comparative outcome of proposed MHS-SCA methodology with existing systems

Method	Accuracy (%)	Specificity (%)	Sensitivity (%)	Precision (%)
2D-CNN model [23]	97.54	98.7	95.5	97
Inception v3 model [24]	98.04	99.25	99.24	96.1
VGG 19 [25]	97.8	99.2	97.32	95.01
MHS-SCA architecture (Proposed model)	99.3	99.4	99.2	99.4

International Journal of Innovative Research of Science, Engineering and Technology (IJIRSET)

Impact Factor 8.699

|www.ijirset.com |A Monthly, Peer Reviewed & Refereed Journal| e-ISSN: 2319-8753| p-ISSN: 2347-6710|

Volume 14, Issue 8, August 2025

|DOI: 10.15680/IJIRSET.2025.1408061|

V. CONCLUSION

Deep learning algorithm can aid healthcare workers in detecting COVID-19 with minimal processing of chest X-ray images. This study summarizes that the detection models built using CNNs with transfer learning technique are able to perform good binary classification tasks on COVID-19 and pneumonia images. COVID-19 and normal CXR images contain similar features which are challenging for the radiologist to interpret. However, the CNN model can easily learn the features in just a few epochs of training and classify the images correctly. The high accuracies obtained suggest that the deep learning models could find something distinctive in the CXR images and that makes the deep networks capable of distinguishing the images correctly. The proposed MHS-SCA Architecture to classify COVID as "NORMAL" or "COVID 19". The proposed MHS-SCA model achieves accuracy (99.3%), precision (99.4), sensitivity (99.2%) and Specificity (99.4%). These trained models can effectively reduce the workload of medical practitioners and increase the accuracy and efficiency of COVID-19 diagnosis.

REFERENCES

1. Daniel, Sir John. "Education and the COVID-19 pandemic." Prospects 49, no. 1 (2020): 91-96.
2. Sevi, Mehmet, and İlhan Aydin. "COVID-19 detection using deep learning methods." In 2020 International conference on data analytics for business and industry: way towards a sustainable economy (ICDABI), pp. 1-6. IEEE, 2020.
3. Ummah, KhanunRoisatul, TitaKarlita, RiyantoSigit, EkoMulyantoYuniarno, I. Ketut Eddy Purnama, and MauridhiHeryPurnomo. "Effect of image pre-processing method on convolutional neural network classification of COVID-19 CT scan images." International Journal of Innovative Computing, Information and Control 18, no. 6 (2022): 1895-1912.
4. Singh, Tinku, Suryanshi Mishra, Riya Kalra, Satakshi, Manish Kumar, and Taehong Kim. "COVID-19 severity detection using chest X-ray segmentation and deep learning." Scientific Reports 14, no. 1 (2024): 19846.
5. Huang, Mei-Ling, and Yu-Chieh Liao. "A lightweight CNN-based network on COVID-19 detection using X-ray and CT images." Computers in Biology and Medicine 146 (2022): 105604.
6. Kumar, Bangaru Siva, and G. SasiBhushana Rao. "CNN-BASED AUTOMATIC DETECTION OF COVID-19 INFECTION USING CHEST X-RAY IMAGES." (2019).
7. Lamsal, Rabindra. "Design and analysis of a large-scale COVID-19 tweets dataset." applied intelligence 51, no. 5 (2021): 2790-2804.
8. Tabik, Siham, Anabel Gómez-Ríos, José Luis Martín-Rodríguez, Iván Sevillano-García, Manuel Rey-Area, David Charte, Emilio Guirado et al. "COVIDGR dataset and COVID-SDNet methodology for predicting COVID-19 based on chest X-ray images." IEEE journal of biomedical and health informatics 24, no. 12 (2020): 3595-3605.
9. Heidari, Morteza, SeyedehnafisehMirniaharikandehei, AbolfazlZargariKhuzani, GopichandhDanala, YuchenQiu, and Bin Zheng. "Detecting COVID-19 infected pneumonia from x-ray images using a deep learning model with image preprocessing algorithm." In Medical Imaging 2021: Computer-Aided Diagnosis, vol. 11597, pp. 202-209. SPIE, 2021.
10. Das, Sangita, and SubhrajyotiMaji. "Impact of Comprehensive Data Preprocessing on Predictive Modelling of COVID-19 Mortality." arXiv preprint arXiv:2408.08142 (2024).
11. Li, Yupeng, Dong Zhao, Chao Ma, José Escorcia-Gutierrez, Nojood O. Aljehane, and Xia Ye. "CDRIME-MTIS: An enhanced rime optimization-driven multi-threshold segmentation for COVID-19 X-ray images." Computers in Biology and Medicine 169 (2024): 107838.
12. Sharma, Neeraj, Luca Saba, Narendra N. Khanna, Mannudeep K. Kalra, Mostafa M. Fouda, and Jasjit S. Suri. "Segmentation-based classification deep learning model embedded with explainable AI for COVID-19 detection in chest X-ray scans." Diagnostics 12, no. 9 (2022): 2132.
13. Saygılı, Ahmet. "A new approach for computer-aided detection of coronavirus (COVID-19) from CT and X-ray images using machine learning methods." Applied Soft Computing 105 (2021): 107323.
14. Dhebe, Ramesh, VeelishaJagtap, PritiMunde, and Prof SaumyaSalian. "Covid-19 Detection using X-ray." (2019): 147-53.
15. Gürsoy, Ercan, and Yasin Kaya. "An overview of deep learning techniques for COVID-19 detection: methods, challenges, and future works." Multimedia Systems 29, no. 3 (2023): 1603-1627.
16. Thakur, Samritika, and Aman Kumar. "X-ray and CT-scan-based automated detection and classification of covid-19 using convolutional neural networks (CNN)." Biomedical Signal Processing and Control 69 (2021): 102920.

International Journal of Innovative Research of Science, Engineering and Technology (IJIRSET)

Impact Factor 8.699

|www.ijirset.com |A Monthly, Peer Reviewed & Refereed Journal| e-ISSN: 2319-8753| p-ISSN: 2347-6710|

Volume 14, Issue 8, August 2025

|DOI: 10.15680/IJIRSET.2025.1408061|

17. Zouch, Wassim, DhouhaSagga, Amira Echtioui, RafikKhemakhem, Mohamed Ghorbel, ChokriMhiri, and Ahmed Ben Hamida. "Detection of COVID-19 from CT and chest X-ray images using deep learning models." Annals of Biomedical Engineering 50, no. 7 (2022): 825-835.
18. Hayat, Ahatsham, PreetyBaglat, FábioMendonça, Sheikh Shanawaz Mostafa, and Fernando Morgado-Dias. "Novel comparative study for the detection of COVID-19 using CT scan and chest X-ray images." International Journal of Environmental Research and Public Health 20, no. 2 (2023): 1268.
19. Zheng, Chuangsheng, Xianbo Deng, Qiang Fu, Qiang Zhou, Jiapei Feng, Hui Ma, Wenyu Liu, and Xinggang Wang. "Deep learning-based detection for COVID-19 from chest CT using weak label." MedRxiv (2020): 2020-03.Ik K
20. Cheng, Cindy, Joan Barceló, Allison Spencer Hartnett, Robert Kubinec, and Luca Messerschmidt. "COVID-19 government response event dataset (CoronaNet v. 1.0)." Nature human behaviour 4, no. 7 (2020): 756-768.
21. Sultana, Abida, Md Nahiduzzaman, Sagor Chandro Bakchy, Saleh Mohammed Shahriar, Hasibul Islam Peyal, Muhammad EH Chowdhury, Amith Khandakar, Mohamed Arselene Ayari, Mominul Ahsan, and Julfikar Haider. "A real time method for distinguishing COVID-19 utilizing 2D-CNN and transfer learning." Sensors 23, no. 9 (2023): 4458.
22. Srinivas, Kudipudi, R. Gagana Sri, K. Pravallika, K. Nishitha, and Subba Rao Polamuri. "COVID-19 prediction based on hybrid Inception V3 with VGG16 using chest X-ray images." Multimedia tools and applications 83, no. 12 (2024): 36665-36682.
23. Karacı, Abdulkadir. "VGGCOV19-NET: automatic detection of COVID-19 cases from X-ray images using modified VGG19 CNN architecture and YOLO algorithm." Neural Computing and Applications 34, no. 10 (2022): 8253-8274.

INTERNATIONAL STANDARD SERIAL NUMBER INDIA

INNO SPACE SJIF Scientific Journal Impact Factor

doi cross ref

निस्केयर NISCAIR

INTERNATIONAL JOURNAL OF INNOVATIVE RESEARCH

IN SCIENCE | ENGINEERING | TECHNOLOGY

9940 572 462 6381 907 438 ijirset@gmail.com

www.ijirset.com

Scan to save the contact details